Fully Reconfigurable Fano Resonator on a Silicon Photonic Chip

Lang Zhou, Bin Wang, *Member, IEEE*, Shuang Zheng, and Weifeng Zhang, *Member, IEEE*

***Abstract*— A fully reconfigurable Fano resonator on a silicon photonic chip is reported. The Fano resonator is realized with the use of an add-drop micro-disk resonator (MDR) and a Mach-Zehnder interferometer (MZI). The waveguides at the through and drop ports of the MDR connect to two spiral waveguide arms of the MZI directly. Two independent metallic micro-heaters are incorporated on top of the MDR and the lower arm of the MZI. Thanks to the resonant mode interference between the MDR and the MZI, the Fano resonance occurs. By thermal tuning the resonance coupling between the MDR and the MZI, the generated Fano resonance is fully tunable. In addition to the independent tunable slope rate (SR) and the resonance wavelength, the Fano resonance wavelength can shift while its line shape remains by simultaneously controlling the two micro-heaters. A chip is designed, fabricated and evaluated. The measurement results show that the static Fano resonance has a line shape with an extinction ratio (ER) of 17.1 dB and SR of −13.6 dB/nm. By simultaneously controlling the two micro-heaters, full reconfigurability of the Fano resonance is demonstrated. Thanks to its straightforward configuration, the proposed Fano resonator holds the key advantage in terms of ultra-compactness and fully reconfigurability, which offers a great potential for applications such as on-chip optical switching, modulation and microwave photonics applications.**

***Index Terms*—Fano resonance, micro-disk resonator, full reconfigurability.**

I. Introduction

FANO resonance, arising from the constructive and destructive interference of a narrow discrete resonance with a broad continuum band of states [1], features a sharp asymmetric line shape. This unique property finds wide applications in high-sensitivity sensor [2], low power consumption optical switch [3], nonlinearity-induced nonreciprocal devices [4], high-efficiency optical modulator [5], and ultra-coherent lasers [6]. So far, various material platforms have been reported to realize Fano resonators [7]–[9]. Among these platforms, silicon photonics is becoming one of the most promising photonic integrated platforms for low-cost, high-volume, and reliable large-scale manufacturing [10]. Numerous silicon-based Fano resonators have been implemented, including photonic crystal cavities [11], [12], Bragg waveguide gratings [13], and micro-ring resonator (MRR)-based structures [14].

Recently, much effort has been directed to the study of a dynamically tunable Fano resonance, and considerable approaches have been reported to realize the tunability of the Fano resonance [15]–[18]. However, these tuning approaches are mainly limited to the shifts of the Fano resonance, which cannot realize the independent tuning of the resonance wavelength or the line shape. In different applications, other spectral characteristics, such as line shape and phase response, should be tunable. For example, for low power-consumption optical switching or high-sensitivity sensing, a Fano resonator is required to have a sharp line shape; for high-linearity electro-optic modulation, a high-speed tunability with a sharp line shape is needed [19]; for microwave photonic phase shifting with a small power variation, a gentle line shape but a large phase shift is required [20]. To meet these different needs of various applications, a fully reconfigurable Fano resonator with independent tunable line shape and resonance wavelength is highly preferred.

To realize the fully tunability, Fano resonators based on two-beam interference in an MRR-coupled MZI have been proposed [21], [22]. The key disadvantage is the complex structure, which causes a high power-consumption. From the perspective of a photonic chip, a smaller physical size of an individual device is highly welcomed, since it can elevate the integration density and power efficiency of a chip. Unlike an MRR suffering from scattering loss due to sidewall roughness from two waveguide sidewalls, a micro-disk resonator (MDR) experiences scattering loss only from the outer sidewall. Thus, the MDR can be designed to have a much smaller size and a higher Q-factor, which is of great benefit to the quality of the Fano resonance in terms of the power consumption and bandwidth [23].

To realize a more compact Fano resonator with a lower power cost, recently, we proposed a thermally tunable Fano resonator based on the interference of the resonant modes between an ultra-compact add-drop MDR and an MZI [24]. A p-type-doped microheater is incorporated in the MDR to realize the tunability of the Fano resonance. By applying a direct current (DC) voltage, the Fano resonance is shifted. During the shifting, the line shape of the Fano resonator is also changed. The independent tuning of the resonance wavelength and line shape cannot be achieved.

Manuscript received 1 June 2022; revised 6 July 2022; accepted 7 July 2022. Date of publication 12 July 2022; date of current version 25 July 2022. This work was supported in part by the National Key Research and Development Program of China under Grant 2018YFE0201800, in part by the National Natural Science Foundation of China under Grants 62071042 and 62105028, and in part by China Postdoctoral Science Foundation under Grant 2021M690390. *(Corresponding author: Weifeng Zhang.)*

The authors are with the Radar Research Lab, School of Information and Electronics, Beijing Institute of Technology, Beijing 100081, China, with the Key Laboratory of Electronic and Information Technology in Satellite Navigation, Beijing Institute of Technology, Ministry of Education, Beijing 100081, China, with the Beijing Institute of Technology Chongqing Innovation Center, Chongqing 401120, China, and also with the Chongqing Key Laboratory of Novel Civilian Radar, Chongqing 401120, China (e-mail: lang.zhou@bit.edu.cn; bin_wang@bit.edu.cn; zs_bit@bit.edu.cn; weifeng.zhang@bit.edu.cn).

Digital Object Identifier 10.1109/JPHOT.2022.3190030

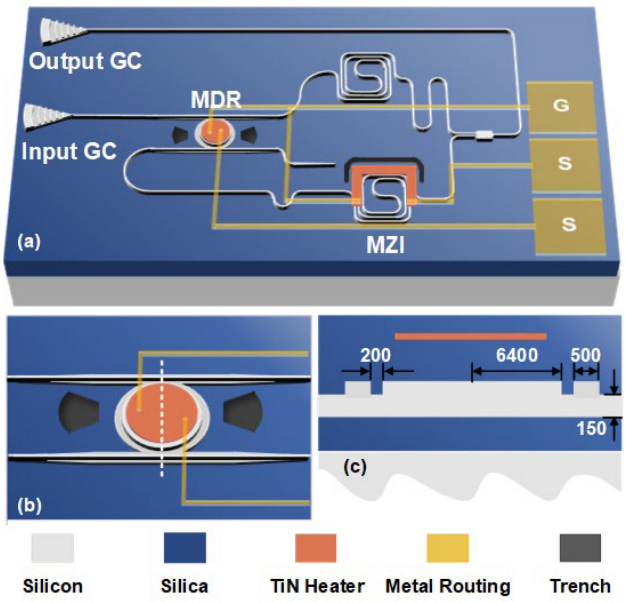

Fig. 1. (a) Perspective view of the proposed Fano resonator. (b) Zoom-in view of the MDR. (c) Cross-sectional view of the MDR along the white dashed line shown in (b) (unit: nm).

To realize a fully tunable Fano resonance, based on our previously reported work, a fully reconfigurable Fano resonator on a silicon photonic chip is proposed. The Fano resonator is realized with the use of an add-drop MDR and an MZI. The waveguides at the through and drop ports of the MDR connect to the two spiral waveguide arms of the MZI directly. Two independent metallic micro-heaters are incorporated on top of the MDR and the lower arm of the MZI. Thanks to the resonant mode interference between the MDR and the MZI, the Fano resonance is produced. By thermal tuning of the resonance wavelength of the MDR and the phase difference between the arms of the MZI, the generated Fano resonance is fully reconfigurable. The resonance wavelength and line shape can be independently tuned. A chip is designed, fabricated and evaluated. The measurement results show that the static Fano resonance has a line shape with an ER of 17.1 dB and SR of −13.6 dB/nm. By simultaneously controlling the two micro-heaters, full reconfigurability of the Fano resonance is demonstrated.

II. Design and Simulation

The perspective view of the proposed Fano resonator is shown in Fig. 1(a). An optical signal is coupled into the chip via an input grating coupler (GC) and sent to an add-drop MDR. The fully etched wire waveguides at the through and drop port connect to the two arms of the MZI directly, and a 2×1 3-dB Multimode interference (MMI) combiner is used to construct the MZI. At the add port, a waveguide terminator is used to minimize the optical reflection from the waveguide end. At the output of the MZI, another GC is used to couple the optical signal out of the chip. Thanks to the resonance interference between the MDR and the MZI, the Fano resonance happens. To minimize the footprint of the MZI, spiral waveguides are employed in the two arms, of which the length difference between the two arms is designed to be 32.4 μm, corresponding to a free spectral range (FSR) of 16.1 nm. By incorporating two micro-heaters on top of the MDR and the lower arm of the MZI, the resonant modes of the MDR and the MZI can be independently tuned, which is of help to tune the resonant mode coupling between the MDR and the MZI, leading to a fully reconfigurable Fano resonance. Fig. 1(b) shows the zoom-in view of the add-drop MDR. To decrease the scattering loss of the confined optical field due to the disk sidewall roughness and enhance the optical coupling between the disk and the bus waveguides, an additional slab waveguide is employed to wrap the disk and the lateral sides of the bus waveguides. Transition tapers are used to connect the rib bus waveguides to fully etched wire waveguides for mode conversion. Since two micro-heaters are used, to reduce the thermal crosstalk, deep trenches are used to surround the MDR and lower arm of the MZI for thermal isolation. The isolation silica layer between the heater and waveguide has a height of 850 nm. Fig. 1(c) shows the cross-sectional view of the MDR along the white dashed line in Fig. 1(b). As can be seen, the radius of the MDR is 6.4 μm and the coupling gap is 200 nm. The width of bus waveguide is set to 0.5 μm for phase-matching condition, which can effectively excite the first-order whispering gallery mode (WGM).

First, a theoretical simulation is performed, in which the spectral response of the proposed Fano resonator is calculated based on the transfer matrix method. The amplitude transmission function of the device can be expressed as

$$T = \left(a_1 \frac{t_1 - t_2 a_{MDR}}{1 - t_1 t_2 a_{MDR}} \sqrt{\gamma} - a_2 \frac{k_1 k_2 \sqrt{a_{MDR}}}{1 - t_1 t_2 a_{MDR}} \sqrt{1-\gamma} \right) \tag{1}$$

where t_i and k_i $(i = 1, 2)$ are the self-coupling and cross-coupling coefficients between the bus and MDR waveguides which satisfy $k_i^2 + t_i^2 = 1$ for lossless coupling, γ is the power ratio of the MMI combiner, a_1 ,a_2, and $a_{MDR}$are the transmission factors of the two arms of MZI, and the MDR. Here, $a_1 = \alpha_1 \exp(j\varphi_1)$, $a_2 = \alpha_2 \exp(j\varphi_2)$, and $a_{MDR} = \alpha_{MDR} \exp(j\theta)$, where α_1, α_2 and α_{MDR} are the amplitude attenuation factors of the two arms of MZI, and the MDR. φ_1 and φ_2 are the phase shift through the MZI arms, respectively. The phase difference of the MZI arms with length difference of L can be expressed as $\varphi = \varphi_1 - \varphi_2 = \exp(j\beta_w L)$, where β_w is the propagation constant of the wire waveguide. $\theta = (j\beta_{MDR} 2\pi R)$ is the round-trip phase shift of the MDR with the radius of R, where β_{MDR} is the propagation constant of the MDR.

The simulation results are given in Fig. 2. In the design, the micro-heaters on top of the MDR and the lower arm of the MZI are used to tune the resonance wavelength of the MDR and the MZI since the generated heat from the micro-heater increase the waveguide index, equivalent to the increase in the MDR radius and the MZI length difference. Fig. 2(a) shows an asymmetric Fano resonance when the MDR radius and the MZI length different are set to be 6.382 μm and 32.8 μm, respectively. As the radius of the MDR is increased, as shown in Fig.2(b), its resonance wavelength is redshifted, and at the different wavelength the line shape is different since the optical

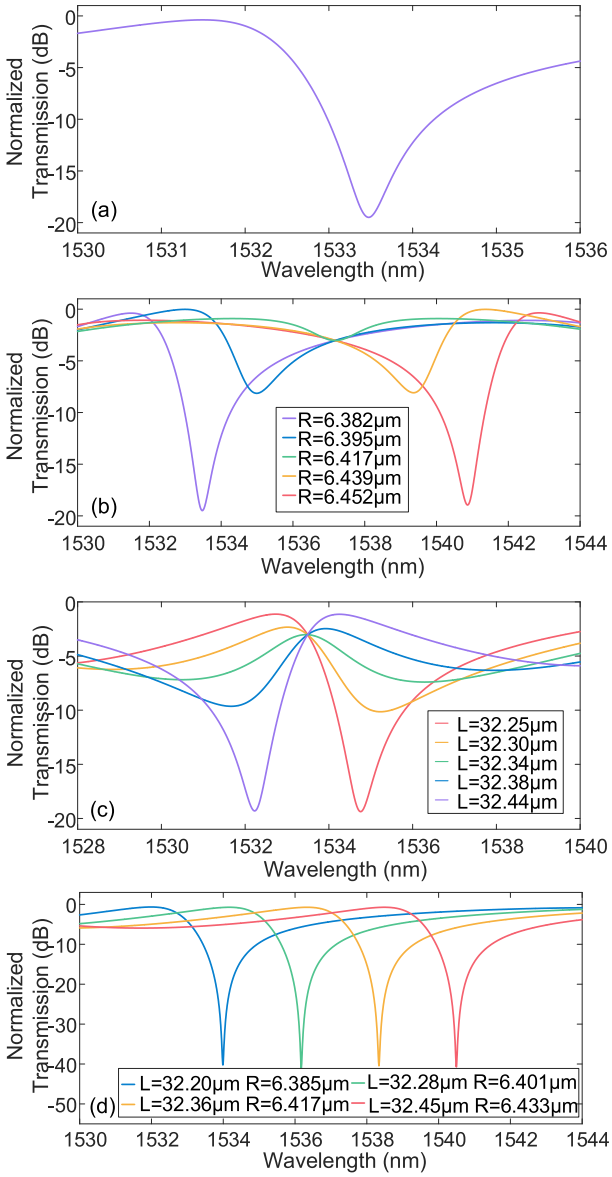

Fig. 2. (a) Simulated Fano resonance of the proposed device. (b) Simulated Fano resonance as the radius of the MDR is increased. (c) Simulated Fano resonance as the length difference of the MZI is increased. (d) Simulated Fano resonance as the radius of the MDR and the length difference of the MZI are increased simultaneously.

interference between the mode of the MDR and MZI is different. It is worth noting when the radius is set to be 6.417 μm, the Fano parameter q is equal to zero, which indicates there is no optical coupling between the MDR and MZI [25], and a resonant notch with a quasi-symmetric line shape is presented. Fig. 2(c) shows the simulated Fano resonance tuning as the length difference of the MZI is increased. During the tuning, the Fano resonance wavelength is unchanged at 1533.5 nm since the resonance wavelength is determined by the MDR. In the meanwhile, the line shape is tuned with different SR and ER. This is because the different resonance wavelength of the tunable MZI leads to different resonant mode coupling. In particular, when the length difference is chosen to be 32.34 μm, the Fano parameter q tends to infinity, which indicates there is no optical coupling between

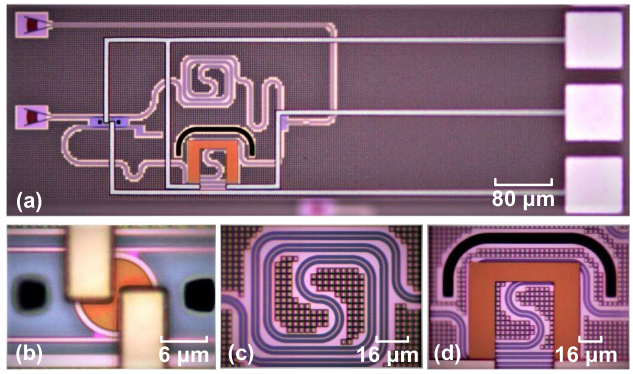

Fig. 3. (a) Image of the fabricated fully reconfigurable Fano resonance captured by a microscope camera. Zoom-in view of (b) the MDR, (c) the upper arm and (d) the lower arm of the MZI.

the MDR and MZI, and a resonant peak with a symmetric line shape is presented. Fig. 2(c) exhibits the simulated Fano resonance as the MDR and MZI are simultaneously tuned. By jointly controlling the MDR and MZI, the generated Fano resonance is redshifted and its line shape remains during the shifting. Thanks to flexible tuning of the MDR and MZI, the proposed Fano resonator features ultra-compactness and full reconfigurability.

III. Fabrication and Characterizations

The proposed Fano resonator is fabricated on a standard SOI wafer with 220-nm-thick top layer and a 2-μm-thick buried oxide (SiO_2) layer. Fig. 3(a) shows the image of the fabricated fully reconfigurable Fano resonator captured by a microscope camera. The two micro-heaters share a ground pad. Fig. 3(b) shows the zoom-in view of the tunable MDR, in which a top-placed micro-heater and deep trenches are observed. Fig. 3(c) gives the zoom-in view of the upper arm of the MZI. To minimize the footprint, the spiral waveguide is used. Fig. 3(d) presents the zoom-in view of the lower arm of the MZI with a top-placed micro-heater. The spiral waveguide is of help to elevate the thermal tuning efficiency. Thanks to the ultra-compactness, the fabricated Fano resonator has a footprint of 432 $\times$ 243 μm^2.

IV. Performance Evaluation

The optical performance of the fabricated Fano resonator is evaluated by measuring its transmission spectrum with the use of an optical vector analyzer (LUNA OVA). A thermoelectric-cooler (TEC) is used to stabilize the room temperature during the test. Fig. 4(a) shows the measured transmission spectrum when the resonator is in the static state. As can be seen, a Fano resonance with an asymmetric line shape is observed with an ER of 17.1 dB and SR of -13.6 dB/nm, corresponding to its q factor of 0.76. The bandwidth of the Fano resonance is 1.15 nm, which is defined as the linewidth of from the peak to the notch resonance [26] . The insertion loss of the device at the resonance peak is around 1 dB exc luding the I/O coupling loss of 12 dB, which is mainly caused by the grating couplers. When a DC voltage is applied to the micro-heater on top of the MDR, the Fano resonance is tuned. When the applied power is increased to

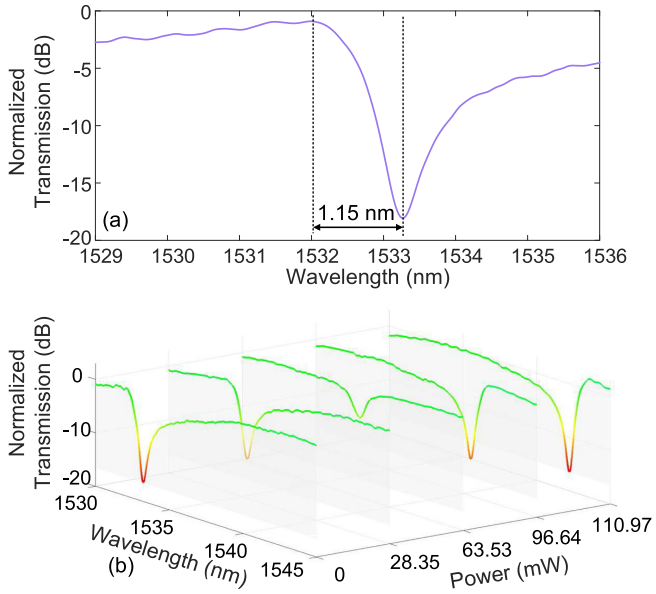

Fig. 4. (a) Measured Fano resonance in the static state. (b) Measured Fano resonance with the increase of the power applied to the micro-heater on top of the MDR.

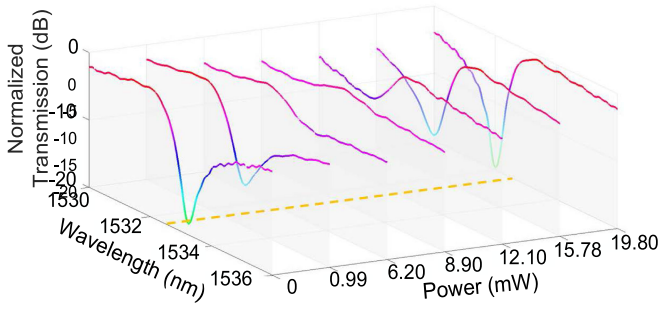

Fig. 5. Measured Fano resonance with the power applied to the micro-heater on top of the lower MZI arm increased. The resonant wavelength of the Fano resonance keeps unchanged.

110.97 mW, the Fano resonance redshifts with a wavelength shift as large as 10.1 nm, and the wavelength shift rate is estimated to be 91.0 pm/mW, as shown in Fig. 4(b). The SR of the line shape is tuned from −13.6 to 13.4 dB/nm, corresponding to the Fano parameter q from 0.76 to −0.74. During the tuning, the ER range is from 5.1 to 18.3 dB. When the applied power is 63.53 mW, a symmetry line shape is generated, which indicates that no optical interference (Fano parameter $q = 0$) occurs between the modes of the MDR and the MZI.

When a DC voltage is applied to the micro-heater on the lower arm of the MZI, the MZI resonance wavelength would be tuned, which leads to the mode coupling change between the MDR and MZI. Therefore, the Fano resonance is tuned in terms of ER and SR. Fig. 5 shows that as the applied power is increased from 0 to 19.80 mW, the Fano resonance wavelength keeps unchanged at 1532.62 nm, and the SR is tuned from −13.6 to 13.5 dB/nm, with the corresponding Fano parameter q tuned from 0.76 to infinity, and then to −0.8. The ER is tuned from 2.1 to 18.9 dB. When the applied power is of 8.90 mW, a symmetric line shape is generated, which indicates that no optical interference

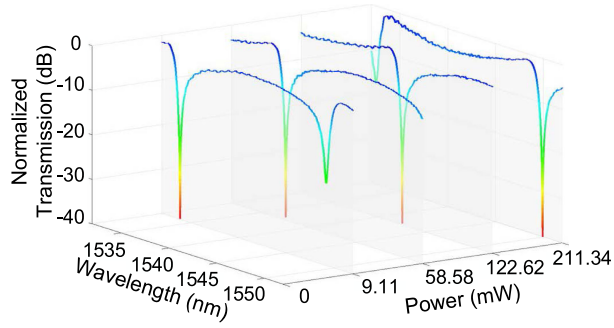

Fig. 6. Measured Fano resonance when the MDR and MZI are simultaneously tuned. The applied power is the total power consumption on the MDR and MZI.

(Fano parameter q tends to infinity) occurs between the modes of the MDR and the MZI, which matches well with the simulation results. The MZI with a top-placed heater on its lower arm has a pi-shift power consumption of 33mW .

When the MDR and MZI are simultaneously tuned, the generated Fano resonance can be fully reconfigured. At the different resonance wavelength, the line shape of the Fano resonance can be tuned to be identical; at a specific resonance wavelength, the line shape of the Fano resonance can be fully tuned. Fig. 6 shows the measured Fano resonance shifting when the MDR and MZI are simultaneously tuned. As can be seen, the Fano resonance is shifted and its line shape maintains, in which the ER is 38.5 dB and the SR is −29.8 dB/nm, corresponding to the Fano parameter q of 0.84. When the total applied power is increased from 9.11 to 211.34 mW, the maximum wavelength shift of the fabricated Fano resonator is measured to be 16.1 nm, and the corresponding wavelength shift rate is calculated to be 79.6 pm/mW. It is worth noting that a sharper Fano line shape with a higher SR can be further achieved by using a higher Q-factor MDR with a larger radius or with a weaker coupling strength between the MDR and the bus waveguides, and a feedback control circuit can also be designed on the chip to improve the stability performance of the Fano resonator.

V. Conclusion

In conclusion, a fully reconfigurable Fano resonator on a silicon photonic chip was demonstrated. The Fano resonator was realized with the use of an add-drop MDR and an MZI. The waveguides at the through and drop ports of the MDR connect to the two spiral waveguide arms of the MZI directly. Two independent metallic micro-heaters are incorporated on top of the MDR and the lower arm of the MZI. An asymmetrical Fano resonant line shape was generated because of the resonant mode interference between the MDR and the MZI. By thermally tuning the MDR and the MZI, the SR and resonance wavelength of the Fano resonance can be independently tunable. Measurement results verified the full reconfigurability of the fabricated Fano resonance. Thanks to its straightforward reconfigurability, the proposed Fano resonator can pave the way for practical applications in low-power consumption optical switching, high-linearity modulation, high-sensitivity sensing, and microwave frequency measurement.

REFERENCES

[1] B. Luk'yanchuk *et al.*, "The Fano resonance in plasmonic nanostructures and metamaterials," *Nature Mater.*, vol. 9, pp. 707–715, Aug. 2010.

[2] Y. Deng, G. Cao, H. Yang, G. Li, X. Chen, and W. Lu, "Tunable and high-sensitivity sensing based on Fano resonance with coupled plasmonic cavities," *Sci. Rep.*, vol. 7, Sep. 2017, Art. no. 10639.

[3] S. Zheng, X. Cao, and J. Wang, "Multimode Fano resonances for low-power mode switching," *Opt. Lett.*, vol. 45, no. 4, pp. 1035–1038, Feb. 2020.

[4] M. Cotrufo, S. A. Mann, H. Moussa, and A. Alù, "Nonlinearity-induced nonreciprocity—Part II," *IEEE Trans. Microw. Theory Techn.*, vol. 69, no. 8, pp. 3584–3597, Aug. 2021.

[5] J. Zhang *et al.*, "Generating Fano resonances in a single-waveguide silicon nanobeam cavity for efficient electro-optical modulation," *ACS Photon.*, vol. 5, no. 11, pp. 4229–4237, Oct. 2018.

[6] Y. Yu, A. Sakanas, A. R. Zali, E. Semenova, K. Yvind, and J. Mørk, "Ultra-coherent Fano laser based on a bound state in the continuum," *Nature Photon.*, vol. 15, pp. 758–764, Aug. 2021.

[7] W. Zhou *et al.*, "Progress in 2D photonic crystal Fano resonance photonics," *Prog. Quantum Electron.*, vol. 38, no. 1, pp. 1–74, Jan. 2014.

[8] M. Rahmani, B. Luk'yanchuk, and M. Hong, "Fano resonance in novel plasmonic nanostructures," *Laser Photon. Rev.*, vol. 7, no. 3, pp. 329–349, Jul. 2013.

[9] X. Wang, J. Duan, W. Chen, C. Zhou, T. Liu, and S. Xiao, "Controlling light absorption of graphene at critical coupling through magnetic dipole quasi-bound states in the continuum resonance," *Phys. Rev. B*, vol. 102, Oct. 2020, Art. no. 155432.

[10] M. Hochberg and T. Baehr-Jones, "Towards fabless silicon photonics," *Nature Photon.*, vol. 4, pp. 492–494, Aug. 2010.

[11] Y. Yua *et al.*, "Fano resonance control in a photonic crystal structure and its application to ultrafast switching," *Appl. Phys. Lett.*, vol. 105, no. 6, Jul. 2014, Art. no. 061117.

[12] S. Fan, "Sharp asymmetric line shapes in side-coupled waveguide-cavity systems," *Appl. Phys. Lett.*, vol. 80, no. 6, pp. 908–910, Feb. 2002.

[13] Z. Zhang *et al.*, "Conversion between EIT and Fano spectra in a microring-Bragg grating coupled-resonator system," *Appl. Phys. Lett.*, vol. 111, no. 8, Jun. 2017, Art. no. 081105.

[14] L. Gu *et al.*, "A compact structure for realizing Lorentzian, Fano, and electromagnetically induced transparency resonance lineshapes in a microring resonator," *Nanophotonics*, vol. 8, no. 5, pp. 841–848, Mar. 2019.

[15] L. Zhou and A. W. Poon, "Fano resonance-based electrically reconfigurable add–drop filters in silicon microring resonator-coupled Mach–Zehnder interferometers," *Opt. Lett.*, vol. 32, no. 7, pp. 781–783, Apr. 2007.

[16] S. Zheng *et al.*, "Compact tunable electromagnetically induced transparency and Fano resonance on silicon platform," *Opt. Exp.*, vol. 25, no. 21, pp. 25655–25662, Oct. 2017.

[17] W. Zhang, W. Li, and J. Yao, "Optically tunable Fano resonance in a grating-based Fabry–Perot cavity-coupled microring resonator on a silicon chip," *Opt. Lett.*, vol. 41, no. 11, pp. 2474–2477, Jun. 2016.

[18] G. Zhao *et al.*, "Tunable Fano resonances based on microring resonator with feedback coupled waveguide," *Opt. Exp.*, vol. 24, no. 18, pp. 20187–20195, Sep. 2016.

[19] S. Chen, G. Zhou, L. Zhou, L. Lu, and J. Chen, "High-linearity Fano resonance modulator using a microring-assisted Mach–Zehnder structure," *J. Lightw. Technol.*, vol. 38, no. 13, pp. 3395–3403, Feb. 2020.

[20] A. Pandey and S. K. Selvaraja, "Fano resonance assisted tunable microwave photonic phase shifter in loaded ring resonator," in *Proc. Conf. Lasers Electro-Opt.*, 2018, pp. 1–2.

[21] X. Liu, Y. Yu, and X. Zhang, "Tunable Fano resonance with a high slope rate in a microring-resonator-coupled Mach–Zehnder interferometer," *Opt. Lett.*, vol. 44, no. 2, pp. 251–254, Jan. 2019.

[22] T. Hu *et al.*, "Tunable Fano resonances based on two-beam interference in microring resonator," *Appl. Phys. Lett.*, vol. 102, no. 1, Dec. 2013, Art. no. 011112.

[23] W. Zhang and J. Yao, "Silicon-based single-mode on-chip ultracompact microdisk resonators with standard silicon photonics foundry process," *J. Lightw. Technol.*, vol. 35, no. 20, pp. 4418–4424, Oct. 2017.

[24] W. Zhang and J. Yao, "Thermally tunable ultracompact Fano resonator on a silicon photonic chip," *Opt. Lett.*, vol. 43, no. 21, pp. 5415–5418, Nov. 2018.

[25] M. F. Limonov, M. V. Rybin, A. N. Poddubny, and Y. S. Kivshar, "Fano resonances in photonics," *Nature Photon.*, vol. 11, pp. 543–554, Nov. 2017.

[26] N. Verellen *et al.*, "Plasmon line shaping using nanocrosses for high sensitivity localized surface plasmon resonance sensing," *Nano Lett.*, vol. 11, pp. 391–397, Jan. 2011.